MATHEMATICAL COMMUNICATIONS
Math. Commun. **17**(2012), 673–696

Measure of long segments intersecting both sides of a Kite as a basis for arbitrary pairs of segments

Roger Böttcher[1,*]

[1] *Händelstr. 1, D-67061 Ludwigshafen am Rhein, Germany*

Received January 18, 2012; accepted July 11, 2012

Abstract. Geometrical probabilities concerning randomly placed segments in relation to certain objects are based on translation-invariant measures of sets containing all appropriate configurations of the moveable segments. Hence it is an advantage to have far reaching sets and measures of elementary events of such type. Here we consider a set of segments that intersect both sides of a so-called "Kite" which consists itself of two symmetrically positioned segments. This result is sufficient to cover all measures of segments that intersect a pair of two arbitrary placed segments in the plane.

AMS subject classifications: 52A22, 60D05

Key words: principle of inclusion-exclusion, invariant measure, geometrical probability

1. Introduction

Since Buffon's investigation of a tossing needle hitting randomly a pattern of parallels in 1777 there is an intriguing attraction proceeding from geometric probabilities. It is our aim to initiate a new point of view to cope with problems of this type. In the outlook of the study [1] the idea is presented to provide a rich amount of geometric probabilities in form of a "modular assembly concept". In the first step it contains only a small number of sufficient "basic measures" which in a second step can be combined – applying the principle of inclusion-exclusion, here abbreviated to PIE – to complex geometrical structures. The research papers [2] and [3] make some further progress in this direction.

Due to these achievements, it is of great value to produce some more elementary measures in the sort of [6], Chapter 6, p.89, considering segments hitting both sides of an angle. Here we are looking for the set T of all segments $\mathcal{S}$ of constant length in the plane intersecting both sides of a so-called "Kite" $\mathcal{K}$, see Figure 1, consisting of two axially symmetric segments $\mathcal{K}_1$, $\mathcal{K}_2$, called components of the Kite. The measure of this set T is an excellent basis to derive much more measurements of this type simply with the help of the principle of inclusion-exclusion (PIE).

We start with an embedding of the Kite in a Cartesian coordinate system and the appellation of points and distances which are frequently used in the further calculations.

*Corresponding author. *Email address:* `Roger.Boettcher@FernUni-Hagen.de` (R. Böttcher)

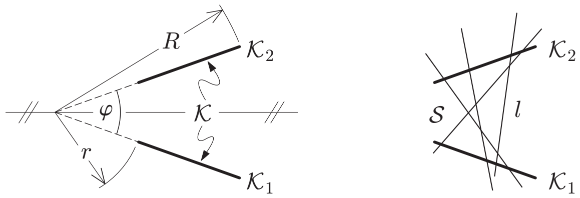

Figure 1: *A Kite $\mathcal{K}$ consisting of two fixed segments $\mathcal{K}_1$ and $\mathcal{K}_2$: $\mathcal{K} = \mathcal{K}_1 \cup \mathcal{K}_2$ (left) and a Kite with some moveable segments $\mathcal{S} \in T$ of length l cutting both components of it (right)*

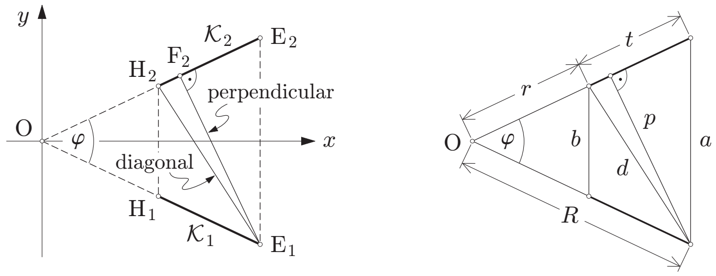

Figure 2: *An embedding of a Kite in Cartesian coordinates: Notation of points and distances*

Definition 1. *A* Kite $\mathcal{K}$ *consists of two axially symmetric segments $\mathcal{K}_1$, $\mathcal{K}_2$ of length $t := R - r$ with $R > 0$, $r \geq 0$ and $R \geq r$. The prolongations of the segments $\mathcal{K}_1$ and $\mathcal{K}_2$ form the angle $0 \leq \varphi \leq \pi$. The set T contains all moveable segments $\mathcal{S}$ of length $l \geq 0$ in the plane that intersect both components of the Kite. We introduce the parameters $\lambda := \frac{l}{R}$ as a relative length and $\eta := \frac{r}{R}$ as a related radius, respectively.*

The following table summarizes the notations for a Kite $\mathcal{K}$ and segments $\mathcal{S}$ and lists some definitions and obvious relationships between them which we are going to use frequently.

Symbol	Condition, Formula	Meaning
O	-	zenith of Kite $\mathcal{K}$
E, H, F	-	vertices and foot of perpendiculars (indices 1, 2)
φ	$0 \leq \varphi \leq \pi$	angle of the Kite $\mathcal{K} : \varphi = \measuredangle(\mathcal{K}_1, \mathcal{K}_2)$
R	$R > 0$	length of the sides $\overline{\mathrm{OE}_1}$, $\overline{\mathrm{OE}_2}$
r	$r \geq 0$	length of the sides $\overline{\mathrm{OH}_1}$, $\overline{\mathrm{OH}_2}$
t	$t = R - r \geq 0$	length of the segments $\mathcal{K}_1$ und $\mathcal{K}_2$
a	$a = 2R \sin \frac{\varphi}{2}$	distance of the ending $\overline{\mathrm{E}_1\mathrm{E}_2}$
b	$b = 2r \sin \frac{\varphi}{2}$	distance of the beginning $\overline{\mathrm{H}_1\mathrm{H}_2}$
d	$d^2 = R^2 + r^2 - 2Rr \cos \varphi$	length of the diagonals $\overline{\mathrm{E}_1\mathrm{H}_2}$, $\overline{\mathrm{E}_2\mathrm{H}_1}$
p	$p = R \sin \varphi$	length of the chords vertex-foot $\overline{\mathrm{E}_1\mathrm{F}_2}$, $\overline{\mathrm{E}_2\mathrm{F}_1}$
l	$l \geq 0$	length of the segments $\mathcal{S}$
λ	$\lambda = \frac{l}{R} \geq 0$	parameter of length or relative length
η	$0 \leq \eta = \frac{r}{R} \leq 1$	related radius

Table 1: *Notation for a Kite $\mathcal{K}$ and segments $\mathcal{S}$*

2. Moving segments and case distinctions

2.1. Moving segments

2.1.1. Density of segments in extended polar coordinates

Analogously to the Kite which is related to Cartesian coordinates we need further coordinates to embed the moving segments $\mathcal{S}$. With respect to the references [1] or [6] the kinematic density

$$dS \;=\; d\zeta \wedge d\rho \wedge d\theta \tag{1}$$

becomes very convenient in extended polar coordinates θ-ρ-ζ, see Figure 3 on the left-hand side: The segment is determined by the angle θ of the normal with the x axis, by its distance ρ to the origin, and by the distance ζ of its left vertex S to the normal.

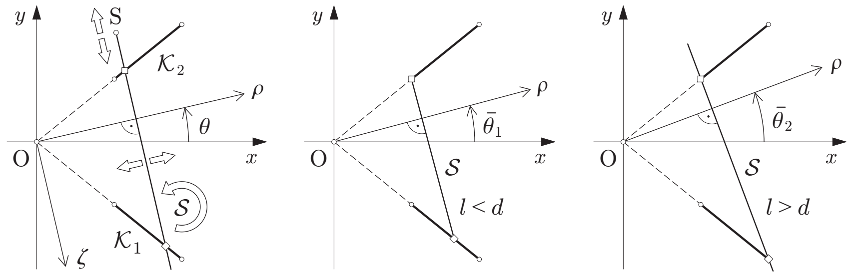

Figure 3: *Kite $\mathcal{K}$ in x-y-coordinates and segments $\mathcal{S}$ with vertex S in θ-ρ-ζ-coordinates (left). Two maxima for rotation of a segment $\mathcal{S}$ keeping it in touch with both components of $\mathcal{K}$ marked by the angles $\bar{\theta}_1$ for the case $l < d$ and $\bar{\theta}_2$ for $l > d$, respectively (centre and right)*

Using these coordinates a set M of segments in the plane can be grasped in form of

$$M \;=\; \big\{\mathcal{S} \mid \theta_1 \le \theta < \theta_2 \;\wedge\; \rho_1 \le \rho < \rho_2 \;\wedge\; \zeta_1 \le \zeta < \zeta_2\big\} \tag{2}$$

and via the kinematic density (1) measured by the definite integral

$$\mu(M) \;=\; \int_M dS \;=\; \int_{\theta=\theta_1}^{\theta_2}\int_{\rho=\rho_1}^{\rho_2}\int_{\zeta=\zeta_1}^{\zeta_2} d\zeta \wedge d\rho \wedge d\theta. \tag{3}$$

2.1.2. Exploitation of the axial symmetry

For any angle $0 \le \theta < \pi$ we have to fix all the positions of a segment $\mathcal{S}$ cutting both components of a given Kite $\mathcal{K}$. The centre and right part of Figure 3 shows that there are case dependent maxima for this angle, which are denoted by $\bar{\theta}_1$ and $\bar{\theta}_2$:

$$0 \;\le\; \theta \;\le\; \bar{\theta}_{1,2} \;\;\text{(where } \bar{\theta}_{1,2} \text{ means } \bar{\theta}_1 \text{ for } l \le d \text{ and } \bar{\theta}_2 \text{ for } l > d\text{, respectively)}, \tag{4}$$

i.e. segments with θ-coordinate of $\bar{\theta}_{1,2} < \theta \le \frac{\pi}{2}$ cannot hit both sides of the Kite[‡]. Additionally, all positions of segments $\mathcal{S}$ related to the Kite $\mathcal{K}$ for angles θ^* of $\frac{\pi}{2} < \theta^* \le \pi$ are derivable due to reflection along the x axis, i.e. for angles $\theta = \pi - \theta^*$.

[‡]The case of $r = 0$ and segments passing through the origin is inconsiderable, since this set of segments is of zero measure.

Hence the set T of all segments $\mathcal{S}$ having two points in common with the Kite $\mathcal{K}$ is the unification of two sets T' and T'' of the same measure. That means we have

$$\begin{aligned} T &= \{\mathcal{S} \mid \#(\mathcal{S}\cap\mathcal{K}) = 2\} = T' \cup T'' \text{ with} \\ T' &= \{\mathcal{S} \mid \#(\mathcal{S}\cap\mathcal{K}) = 2 \wedge 0 \le \theta \le \bar\theta_{1,2}\} \text{ and} \\ T'' &= \{\mathcal{S} \mid \#(\mathcal{S}\cap\mathcal{K}) = 2 \wedge \pi - \bar\theta_{1,2} \le \theta \le \pi\} \end{aligned}$$

so that $\mu(T') = \mu(T'')$, $\mu(T' \cap T'') = 0$, and eventually $\mu(T) = 2\cdot\mu(T')$. Thus, to calculate the measure $\mu(T)$ it is sufficient to look only for the set T'.

2.1.3. Functions related to exposed segments

To gain the set T' we introduce some helpful functions which characterize some segments in particular positions related to a given Kite.

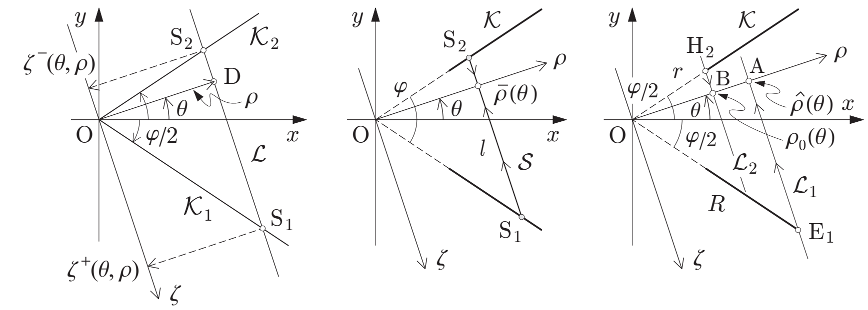

Figure 4: *(left) Distances $\zeta^-(\theta,\rho)$, $\zeta^+(\theta,\rho)$, (centre) $\bar\rho(\theta)$, and (right) $\hat\rho(\theta)$, $\rho_0(\theta)$*

Lemma and Definition 1. *Let $\mathcal{L}$ be a line determined by its distance ρ from the origin and the angle $0 \le \theta \le \bar\theta_{1,2}$ of its normal with the x axis (Figure 4 on the left), where the angles $\bar\theta_{1,2}$ are according to (4). Then the coordinates ζ of the two points S_1 and S_2 of intersection with the half-lines of an angle $\varphi = \measuredangle(\mathcal{K}_1,\mathcal{K}_2)$ are*

$$[0,\bar\theta_{1,2}[\times\mathbb{R}^+ \longrightarrow \mathbb{R} : (\theta,\rho) \longmapsto \zeta(\mathrm{S}_1) = +\rho\cdot\tan(\theta+\tfrac{\varphi}{2}) =: \zeta^+(\theta,\rho)\,, \quad (5)$$
$$[0,\bar\theta_{1,2}[\times\mathbb{R}^+ \longrightarrow \mathbb{R} : (\theta,\rho) \longmapsto \zeta(\mathrm{S}_2) = -\rho\cdot\tan(\tfrac{\varphi}{2}-\theta) =: \zeta^-(\theta,\rho)\,. \quad (6)$$

Proof. The ζ-intercepts ζ^+ and ζ^- of the points S_1 and S_2, respectively, due to the extended polar coordinates are quickly derivable according to the right-angled triangles $\triangle\mathrm{FOS}_1$ and $\triangle\mathrm{FOS}_2$, respectively, see Figure 4 on the left-hand side. □

The centre and right part of Figure 4 motivate to fix further particular distances:

Lemma and Definition 2. *Consider a segment $\mathcal{S}$ of length l that vertices S_1 and S_2 are touching both the sides of a Kite $\mathcal{K}$, see centre of Figure 4. Then its distance from the origin is a function of the θ coordinate of the segment:*

$$[0,\bar\theta_{1,2}[\longrightarrow \mathbb{R} : \theta \longmapsto \rho(\overline{\mathrm{S}_1\mathrm{S}_2} = l) = \frac{l}{2}\cdot\frac{\cos 2\theta + \cos\varphi}{\sin\varphi} =: \bar\rho(\theta)\,. \quad (7)$$

Proof. Using relations (5) and (6) due to Lemma 1 we have the condition

$$\zeta^{+}(\theta,\bar\rho)-\zeta^{-}(\theta,\bar\rho) \;=\; \bar\rho\cdot\big(\tan(\theta+\tfrac{\varphi}{2})+\tan(\tfrac{\varphi}{2}-\theta)\big) \overset{!}{=} l\,. \qquad (*)$$

With tan = sin / cos and the addition formulas for the sine and cosine the factor on the left-hand side of the expression $\bar\rho$ can be converted to

$$\frac{\sin(\frac{\varphi}{2}+\theta)}{\cos(\frac{\varphi}{2}+\theta)}+\frac{\sin(\frac{\varphi}{2}-\theta)}{\cos(\frac{\varphi}{2}-\theta)} \;=\; \frac{\frac{1}{2}\sin\frac{\varphi}{2}\,\cos\frac{\varphi}{2}}{\cos(\frac{\varphi}{2}+\theta)\cos(\frac{\varphi}{2}-\theta)} \;=\; \frac{\sin\varphi}{\frac{1}{2}\,(\cos 2\theta+\cos\varphi)}.$$

Within the formula (*) we get the asserted function (7): $\bar\rho(\theta) = \frac{l}{2}\cdot(\cos 2\theta + \cos\varphi)/\sin\varphi$. □

Lemma and Definition 3. *If a line $\mathcal{L}_1$ is passing through the point* E_1 *and another one $\mathcal{L}_2$ through the point* H_2 *of a Kite $\mathcal{K}$ (see Figure 4, right), then the distances from the origin to the lines are functions of the polar coordinate θ of these lines:*

$$[0,\bar\theta_{1,2}[\;\longrightarrow\mathbb{R}\,:\,\theta\longmapsto\rho(\mathrm{E}_1\in\mathcal{L}_1) \;=\; R\cdot\cos(\theta+\tfrac{\varphi}{2}) \;=:\; \hat\rho(\theta) \;\; \textit{and} \qquad (8)$$
$$[0,\bar\theta_{1,2}[\;\longrightarrow\mathbb{R}\,:\,\theta\longmapsto\rho(\mathrm{H}_2\in\mathcal{L}_2) \;=\; r\cdot\cos(\tfrac{\varphi}{2}-\theta) \;=:\; \rho_0(\theta)\,. \qquad (9)$$

Proof. This follows immediately due to the right-angled triangles $\triangle\mathrm{E}_1\mathrm{AO}$ and $\triangle\mathrm{OBH}_2$ with hypotenuses of length R and r, respectively, see Figure 4 on the right hand side. □

To fix all the moving segments $\mathcal{S}$ intersecting both sides of a Kite $\mathcal{K}$ we shall introduce two further angles of special meaning. For their motivation see Figure 5: To keep the vertices of a rotating segment $\mathcal{S}$ in touch with both components $\mathcal{K}_1$ and $\mathcal{K}_2$ of a Kite, these angles mark each the beginning when vertex on the right-hand side according to the direction of the normal has to leave the point E_1.

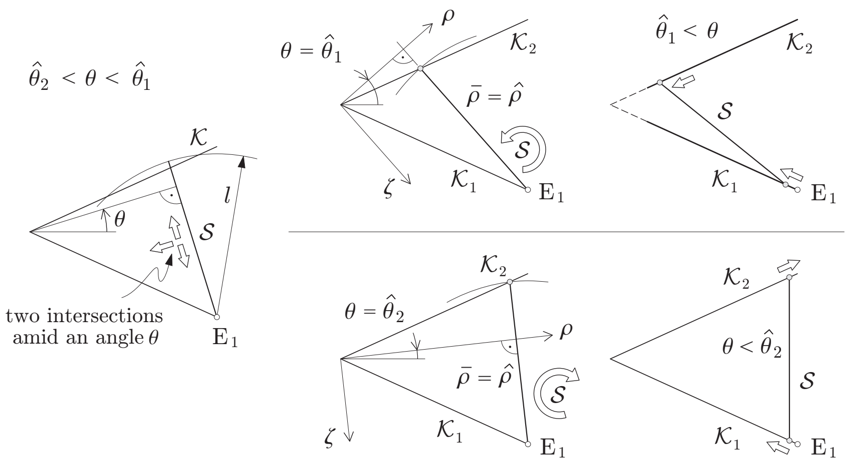

Figure 5: *The incidences of angles $\hat\theta_1$ and $\hat\theta_2$*

The formal definition of these angles and their dependencies of the size of the segment and the Kite are summarized in the following lemma:

Lemma and Definition 4. *Let $\mathcal{K}$ be a Kite with angle $0 \le \varphi \le \pi$ and parameters a, d, and p according to Tab. 1 and $\mathcal{S}$ be a segment of length l with $p < l < \min(a, d)$. The angles $\hat{\theta}_1$ and $\hat{\theta}_2$ respectively are defined as the θ coordinate of the segment $\mathcal{S}$, if one vertex of $\mathcal{S}$ touches the point E_1 and the other one lies on the component $\mathcal{K}_2$ of the Kite. In other words: If $\hat{\theta}_1$ or $\hat{\theta}_2$ respectively is the angle between the normal of $\mathcal{S}$ and the x axis, then the distance from the origin to the segment $\mathcal{S}$ is $\bar{\rho}(\theta) = \hat{\rho}(\theta) > 0$. Under the condition of $\hat{\theta}_1 \ge \hat{\theta}_2$, these angles are given by*

$$\theta(\overline{\mathrm{S}_1\mathrm{S}_2} = l \,\wedge\, \mathrm{E}_1 \in \mathcal{S}) = \frac{\pi}{2} + \frac{\varphi}{2} - \arcsin\frac{\sin\varphi}{\lambda} \quad =: \; \hat{\theta}_1 \,, \tag{10}$$

$$\theta(\overline{\mathrm{S}_1\mathrm{S}_2} = l \,\wedge\, \mathrm{E}_1 \in \mathcal{S}) = \frac{\varphi}{2} - \frac{\pi}{2} + \arcsin\frac{\sin\varphi}{\lambda} \quad =: \; \hat{\theta}_2 \,, \tag{11}$$

and obviously we have $\hat{\theta}_1 + \hat{\theta}_2 = \varphi$. Remarks: (1) Due to $p < l$ it is well-defined that $\sin\varphi < \lambda$. (2) The angle $\hat{\theta}_2$ does not appear for segments with $l > a$ and the angle $\hat{\theta}_1$ does not occur for $l > d$.

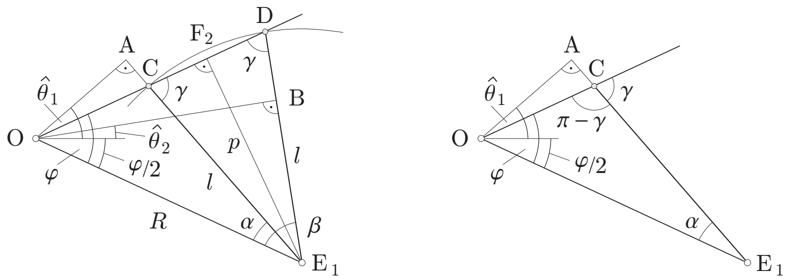

Figure 6: *Auxiliary figures for the calculation of angles $\hat{\theta}_1$ and $\hat{\theta}_2$*

Proof. It is possible to start directly by the analytic expression $\bar{\rho}(\theta) = \hat{\rho}(\theta)$ and after a lot of conversions via trigonometric functions receiving eventually the angles in form of (10) and (11). An analysis of the positions of the segment $\mathcal{S}$ and the Kite $\mathcal{K}$ according to Figure 6 is less algebraic and yields much more insight into the geometry we are interested in. Along this way we find

$$\left(\hat{\theta}_1 + \tfrac{\varphi}{2}\right) + \alpha \;=\; \tfrac{\pi}{2} \qquad \text{and} \qquad \left(\hat{\theta}_2 + \tfrac{\varphi}{2}\right) + \beta \;=\; \tfrac{\pi}{2} \tag{I}$$

for the sums of angles in the right-angled triangles $\triangle\mathrm{WE}_1\mathrm{A}$ and $\triangle\mathrm{WE}_1\mathrm{B}$ creating a relationship between the unknown angles $\hat{\theta}_1$ and $\hat{\theta}_2$ to two other ones: namely α and β which are easy to calculate. Now the triangle $\triangle\mathrm{CE}_1\mathrm{D}$ is an isosceles one, has the sum of angles $2\gamma + \beta - \alpha = \pi$, and due to the – except of orientation – congruent triangles $\triangle\mathrm{CE}_1\mathrm{F}_1$ and $\triangle\mathrm{DE}_1\mathrm{F}_1$ we have for the angle γ the formula

$$\gamma \;=\; \arcsin\frac{s}{l} \;=\; \arcsin\frac{R\sin\varphi}{l} \;=\; \arcsin\frac{\sin\varphi}{\lambda}\,. \tag{II}$$

In the triangles $\triangle\mathrm{WE}_1\mathrm{C}$ (see also the right part of Figure 6) and $\triangle\mathrm{WE}_1\mathrm{D}$ due to the sums $\varphi + \alpha + (\pi - \gamma) = \pi$ and $\varphi + \beta + \gamma = \pi$ we obtain the expressions

$$\alpha \;=\; \gamma - \varphi \qquad \text{and} \qquad \beta \;=\; \pi - \varphi - \gamma\,. \tag{III}$$

If we transform the relations in (I) and substitute the angles α and β due to (III) and γ due to (II) we receive

$$\hat{\theta}_1 \;=\; \tfrac{\pi}{2} - \tfrac{\varphi}{2} - \alpha \;=\; \tfrac{\pi}{2} + \tfrac{\varphi}{2} - \gamma\,, \quad \hat{\theta}_2 \;=\; \tfrac{\pi}{2} - \tfrac{\varphi}{2} - \beta \;=\; \tfrac{\varphi}{2} - \tfrac{\pi}{2} + \gamma$$

which are the asserted forms (10) and (11). – Eventually we have (see Figure 6 once more): For $l > d$ there is no point C of intersection on the side $\mathcal{K}_2$; analogous the case $l > a$ is responsible for the fact that the point D vanishes on the same component of the Kite. $\square$

Finally, we come back to the angles $\bar{\theta}_{1,2}$ according to the Figure 3 and Figure 7:

Lemma and Definition 5. *It is possible to place a segment $\mathcal{S}$ of length l with $b \le l \le d$ in such a way related to a Kite $\mathcal{K}$ that one vertex of the segment is touching the point* H_2 *while the other one lies on the component $\mathcal{K}_1$, in this case we call the θ polar coordinate of the segment $\bar{\theta}_1$. Similarly a segment $\mathcal{S}$ of length $l \ge d$ is able to connect the points* H_2 *and* E_1 *of the Kite, then the θ polar coordinate is called $\bar{\theta}_2$. For both cases see Figure 7. For these two angles we have the relationships*

$$\theta(\overline{\mathrm{S}_1\mathrm{H}_2} = l \,\wedge\, \mathrm{S}_1, \mathrm{H}_2 \in \mathcal{S}) = \frac{\pi}{2} - \frac{\varphi}{2} - \arcsin\left(\frac{r}{l}\,\sin\varphi\right) \;=:\; \bar{\theta}_1\,, \tag{12}$$

$$\theta(\overline{\mathrm{E}_1\mathrm{H}_2} \le l \,\wedge\, \mathrm{E}_1, \mathrm{H}_2 \in \mathcal{S}) = \frac{\pi}{2} - \frac{\varphi}{2} - \arcsin\left(\frac{r}{d}\,\sin\varphi\right) \;=:\; \bar{\theta}_2 \tag{13}$$

to the length l of the segment and the parameters r, d, and φ to the Kite. – Remark: The arcus functions are well-defined, since inside the interval $0 \le \varphi \le \pi$ we have due to $r\sin\varphi \le b = 2r\sin\frac{\varphi}{2} \le l$ for the first angle the argument $\frac{r}{l}\sin\varphi \le 1$. And in the second case we have due to $r \le R$ and the cosine law the inequality $r\sin\varphi \le d$, i.e. once more the validity $\frac{r}{d}\sin\varphi \le 1$.

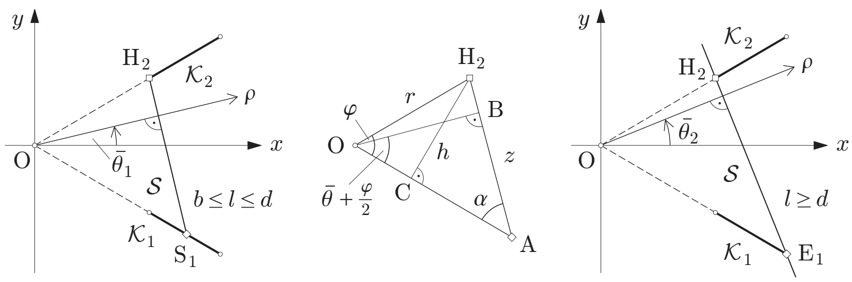

Figure 7: *The angles $\bar{\theta}_1$ and $\bar{\theta}_2$*

Proof. The left and right part respectively of Figure 7 depicts the occurrences of the angles $\bar{\theta}_1$ and $\bar{\theta}_2$. Due to the triangle $\triangle\mathrm{H}_2\mathrm{OA}$ and the inscribed right-angled triangles we obtain immediately the relation $\triangle\mathrm{BOA} : \bar{\theta} = \frac{\pi}{2} - \frac{\varphi}{2} - \alpha$ as well as $\triangle\mathrm{H}_2\mathrm{OC} : h = r\sin\varphi$, so that $\triangle\mathrm{AH}_2\mathrm{C} : \sin\alpha = \frac{h}{z} = \frac{r}{z}\sin\varphi$ and hence

$$\bar{\theta} \;=\; \tfrac{\pi}{2} - \tfrac{\varphi}{2} - \arcsin\left(\tfrac{r}{z}\sin\varphi\right).$$

Eventually, we receive for $z = l$ and for point A becomes the vertex S_1 the angle $\bar{\theta}_1 = \bar{\theta}$ and for $z = d$ and for $\mathrm{A} = \mathrm{E}_1$ the second angle $\bar{\theta}_2 = \bar{\theta}$. $\square$

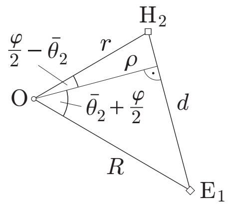

Figure 8: *Alternative expression for $\bar\theta_2$ to (13)*

Remark 1. *There is an alternative formula for the angle $\bar\theta_2$ avoiding the usage of the length d and instead of this requiring only the radii R, r, and the related one $\eta = \frac{r}{R}$, respectively. To receive this expression following the Figure 8 and assert the equality*

$$\rho_0(\bar\theta_2) = r\cos(\tfrac{\varphi}{2} - \bar\theta_2) = R\cos(\bar\theta_2 - \tfrac{\varphi}{2}) = \hat\rho(\bar\theta_2)$$

for the ρ-coordinates (9) and (8) in this case. An application of the addition formula for the cosine function gives

$$\begin{aligned} (1+\eta)\sin\tfrac{\varphi}{2}\sin\bar\theta_2 \;&=\; (1-\eta)\cos\tfrac{\varphi}{2}\cos\bar\theta_2 \qquad (14)\\ \Rightarrow\ \tan\bar\theta_2 \;&=\; \tfrac{1-\eta}{1+\eta}\cot\tfrac{\varphi}{2} \Rightarrow \bar\theta_2 \;=\; \tfrac{\pi}{2} - \operatorname{arccot}\big(\tfrac{1-\eta}{1+\eta}\cot\tfrac{\varphi}{2}\big)\,. \end{aligned}$$

Herewith all the information is gathered to describe a rotating segment with the angle θ between its normal and the x axis from 0 to $\bar\theta_{1,2}$ related to a Kite. This brings us next to the necessary case distinctions.

2.2. Case distinctions

2.2.1. Geometric relations of segments to the Kite

Concerning the relations between the length l of a segment $\mathcal{S}$ and the geometry of a Kite $\mathcal{K}$ we have the following case distinctions, see the boundaries in Figures 9 and 10:

$$(\mathbf{0}):\quad 0 \le l \le b \;\Leftrightarrow\; 0 \le \lambda \le 2\eta\sin\tfrac{\varphi}{2}\,,$$

$$(\mathbf{1}):\begin{cases} b < l \le p \;\Leftrightarrow\; 2\eta\sin\tfrac{\varphi}{2} < \lambda \le \sin\varphi & \text{for } 0 \le \varphi < \bar\varphi,\\ b < l \le d \;\Leftrightarrow\; 2\eta\sin\tfrac{\varphi}{2} < \lambda \le \Phi & \text{for } \bar\varphi \le \varphi \le \pi, \end{cases}$$

$$(\mathbf{2.1}): a < l \le d \Leftrightarrow 2\sin\tfrac{\varphi}{2} < \lambda \le \Phi \quad (\text{for } 0 \le \varphi \le \hat\varphi),$$

$$(\mathbf{2.2}): p < l \le \min(a, d \Leftrightarrow \sin\varphi < \lambda \le \min(2\sin\tfrac{\varphi}{2}, \Phi) \quad (\text{for } 0 \le \varphi \le \bar\varphi),$$

$$(\mathbf{2.3}): d < l \le a \Leftrightarrow \Phi < \lambda \le 2\sin\tfrac{\varphi}{2} \quad (\text{for } \hat\varphi \le \varphi \le \pi),$$

$$(\mathbf{3}): \max(a, d) < l \;\Leftrightarrow\; \max(2\sin\tfrac{\varphi}{2}, \Phi) < \lambda.$$

In the case distinctions ($\mathbf{c}$) above the following symbols for short are used:

$$\Phi := \tfrac{d}{R} = \sqrt{1+\eta^2 - 2\eta\cos\varphi}\,,\;\; \bar\varphi := \arccos\eta\,,\;\; \hat\varphi := \arccos\big(\tfrac{1}{2}\cdot(1+\eta)\big)$$

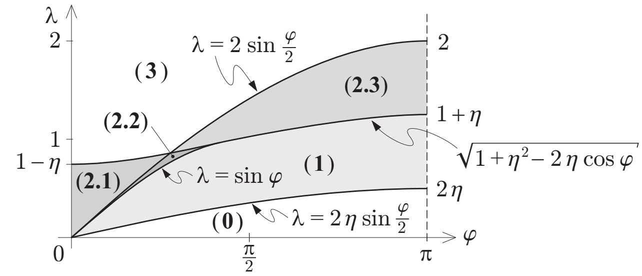

Figure 9: *Case distinctions in the diagram of parameters φ and λ*

where Φ stands for the related length of the diagonal and the angles for partitions of various cases, the latter ones are due to relations (note $R > r$ and $a, d, p \geq 0$):

$$\begin{aligned}
\varphi = \bar{\varphi} : p^2 \;&=\; R^2 \sin^2 \bar{\varphi} = R^2 + r^2 - 2\,R\,r \cos \bar{\varphi} = d^2 \\
&\Rightarrow 0 = R^2 \cos^2 \bar{\varphi} - 2\,R\,r \cos \bar{\varphi} + r^2 \\
&\Rightarrow 0 = (R \cos \bar{\varphi} - r)^2 \quad \Rightarrow \quad \bar{\varphi} = \arccos \eta \quad \text{and} \\
\varphi = \hat{\varphi} : d^2 \;&=\; R^2 + r^2 - 2\,R\,r \cos \hat{\varphi} = 2\,R^2 (1 - \cos \hat{\varphi}) = a^2 \\
&\Rightarrow \quad 2\,R(R-r) \cos \hat{\varphi} = (R-r)(R+r) \quad \Rightarrow \quad \hat{\varphi} = \arccos\left(\tfrac{1}{2} \cdot (1+\eta)\right).
\end{aligned}$$

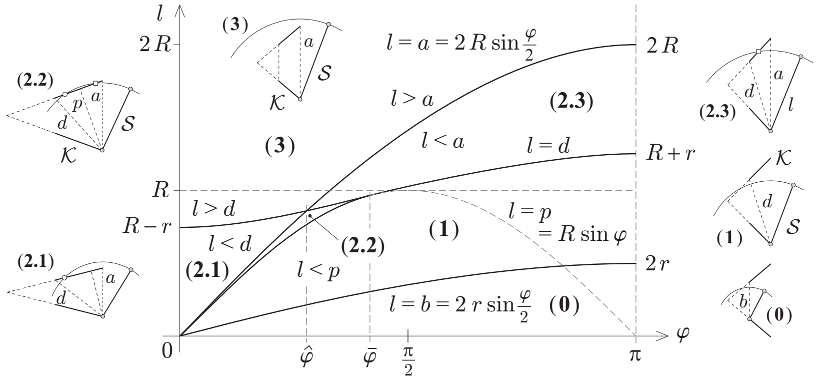

Figure 10: *Case distinctions in the diagram of parameters φ and l with representative examples of a Kite $\mathcal{K}$ and a related segment $\mathcal{S}$ as an auxiliarily visual element*

The boundaries $l = p(\varphi)$ and $l = d(\varphi)$ are tangent to each other for $\varphi = \bar{\varphi}$ where we have $p(\bar{\varphi}) = d(\bar{\varphi}) = \sqrt{R^2 - r^2}$ and $p'(\bar{\varphi}) = p'(\bar{\varphi}) = r$. Especially, there is no further intersection between these boundaries and hence no further case.

2.2.2. The set T' related to the case distinctions

According to the notation (2) for sets of segments we can grasp all the cases $(\mathbf{c}) = (\mathbf{1})$, $(\mathbf{2.1})$, $(\mathbf{2.2})$, $(\mathbf{2.3})$, and $(\mathbf{3})$ in the union

$$T'_{(\mathbf{c})} \;=\; \bigcup_{i=1}^{n_{(\mathbf{c})}} T'_{(\mathbf{c}),i} \;=\; \bigcup_{i=1}^{n_{(\mathbf{c})}} \left\{\, \mathcal{S} \mid b^{\mathrm{l}}_{(\mathbf{c}),i} \,\leq\, \operatorname{epc}(\mathcal{S}) = (\theta, \rho, \zeta) \,<\, b^{\mathrm{u}}_{(\mathbf{c}),i} \,\right\} \qquad (15)$$

of disjoint sets $T'_{(\mathbf{c}),i} \cap T'_{(\mathbf{c}),j} = \emptyset$ for $i \neq j$ where $\operatorname{epc}(\mathcal{S}) = (\theta, \rho, \zeta)$ denotes the extended polar coordinates of a segment $\mathcal{S}$. To keep a segment all the time in touch with both components of the Kite these coordinates in (15) are limited in lower and upper boundaries

$$b^{\mathrm{l,u}}_{(\mathbf{c}),i} = (\,\theta^{\mathrm{l,u}}_{(\mathbf{c}),i}\,,\,\rho^{\mathrm{l,u}}_{(\mathbf{c}),i}\,,\,\zeta^{\mathrm{l,u}}_{(\mathbf{c}),i})$$

due to the case $(\mathbf{c})$ and the modus $i = 1, ..., n_{(\mathbf{c})}$ where the number $n_{(\mathbf{c})} \in \mathbb{N}$ additionally is case distinctive. Table 2 contains all the boundaries using the functions which are asserted within the Section 2.1.3.

case $(\mathbf{c})$	modus i from 1 to $n_{(\mathbf{c})}$	boundary $b^{\mathrm{u}}_{(\mathbf{c}),i}$ and $b^{\mathrm{o}}_{(\mathbf{c}),i}$						type of modus
		θ		ρ		ζ		
		$\theta^{\mathrm{u}}_{(\mathbf{c}),i}$	$\theta^{\mathrm{o}}_{(\mathbf{c}),i}$	$\rho^{\mathrm{u}}_{(\mathbf{c}),i}$	$\rho^{\mathrm{o}}_{(\mathbf{c}),i}$	$\zeta^{\mathrm{u}}_{(\mathbf{c}),i}$	$\zeta^{\mathrm{o}}_{(\mathbf{c}),i}$	
$(\mathbf{1})$	1	0	$\bar{\theta}_1$	ρ_0	$\bar{\rho}$	$\zeta^+ - l$	ζ^-	(e)
$(\mathbf{2.1})$	1	0	$\hat{\theta}_1$	ρ_0	$\hat{\rho}$	$\zeta^+ - l$	ζ^-	(v)
	2	$\hat{\theta}_1$	$\bar{\theta}_1$	ρ_0	$\bar{\rho}$	$\zeta^+ - l$	ζ^-	(e)
$(\mathbf{2.2})$	1	0	$\hat{\theta}_2$	ρ_0	$\bar{\rho}$	$\zeta^+ - l$	ζ^-	(e)
	2	$\hat{\theta}_2$	$\hat{\theta}_1$	ρ_0	$\hat{\rho}$	$\zeta^+ - l$	ζ^-	(v)
	3	$\hat{\theta}_1$	$\bar{\theta}_1$	ρ_0	$\bar{\rho}$	$\zeta^+ - l$	ζ^-	(e)
$(\mathbf{2.3})$	1	0	$\hat{\theta}_2$	ρ_0	$\bar{\rho}$	$\zeta^+ - l$	ζ^-	(e)
	2	$\hat{\theta}_2$	$\bar{\theta}_2$	ρ_0	$\hat{\rho}$	$\zeta^+ - l$	ζ^-	(v)
$(\mathbf{3})$	1	0	$\bar{\theta}_2$	ρ_0	$\hat{\rho}$	$\zeta^+ - l$	ζ^-	(v)

Table 2: *Boundaries for the set T' dependent on case and modus*

Complementarily, the type of the modus is listed; this is the geometric relation when the segment is "starting" (due to the case and θ coordinate) the two intersections with the Kite, see Figure 11. Here (e) stands for an "embrace" with regard to the fact that the segment is embraced by both sides of the Kite, (v) means "vertex" since the segment hits the vertex E_1 starting their motion to stay in two intersections.

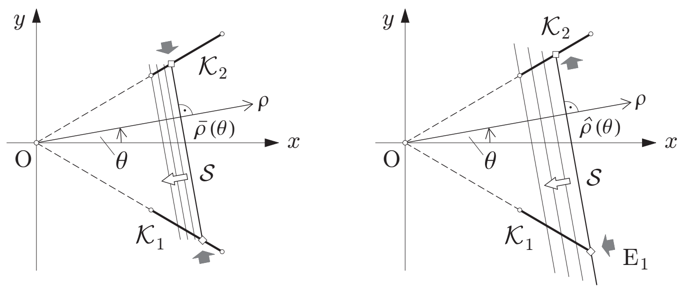

Figure 11: *Type of modus: (e) for "embrace" and (v) for "vertex"*

3. Calculation of the measure $\mu(T)$

Our next step is to integrate the differential form dS in respect to (3). We are going to do this in two steps: First, we set functions which are based on very frequently occurring integrals which afterwards simply can be added. A closer look at the Tab. 2 shows that namely for ζ the range of integration is $[\zeta^+ - l, \zeta^-]$ all the time. And for the coordinate ρ there exist only the intervals $[\rho_0, \bar\rho]$ and $[\rho_0, \hat\rho]$ as ranges for integration. And finally for the coordinate θ we have the values 0, $\hat\theta_1$, $\hat\theta_2$, and $\bar\theta_{1,2}$ respectively as limits for integration.

Lemma and Definition 6. *We state the following definite integrals which are defined as functions f, and $\bar g$, $\hat g$ as well as $\bar h_0$, $\hat h_0$, $\bar h_1$, $\hat h_1$, $\bar h_2$, $\hat h_2$, $\hat h_{21}$-the latter ones are summaries under the notion of here so-called h-functions:*

$$f(l,\varphi;\theta,\rho) := \int_{\zeta^+(\theta,\rho)-l}^{\zeta^-(\theta,\rho)} d\zeta \;=\; l \,+\, \rho\cdot\tan(\theta-\tfrac{\varphi}{2}) \,-\, \rho\cdot\tan(\theta+\tfrac{\varphi}{2}),$$

$$\begin{aligned}\bar g(l,r,\varphi;\theta) &:= \int_{\rho_0(\theta)}^{\bar\rho(\theta)} f(l,\varphi;\theta,\rho)\,d\rho \;=\; \tfrac12\,\csc(\varphi)\cos(\theta-\tfrac{\varphi}{2})\sec(\theta+\tfrac{\varphi}{2})\\ &\quad\times\big[l\,\cos(\theta+\tfrac{\varphi}{2}) - r\,\sin(\varphi)\big]^2,\end{aligned}$$

$$\begin{aligned}\hat g(l,R,r,\varphi;\theta) &:= \int_{\rho_0(\theta)}^{\hat\rho(\theta)} f(l,\varphi;\theta,\rho)\,d\rho \;=\; R\cos(\theta+\tfrac{\varphi}{2})\big[l-\tfrac{R}{2}\,\sec(\theta-\tfrac{\varphi}{2})\sin\varphi\big]\\ &\quad - r\,\cos(\theta-\tfrac{\varphi}{2})\big[l-\tfrac{r}{2}\,\sec(\theta+\tfrac{\varphi}{2})\sin\varphi\big],\end{aligned}$$

$$\begin{aligned}\bar h_0(l,R,r,\varphi) &:= \int_0^{\bar\theta_1} \bar g(l,r,\varphi;\theta)\,d\theta \;=\; \tfrac18\,l^2\,\csc(\varphi)\big[2\,\bar\theta_1\cos\varphi+\sin(2\,\bar\theta_1)\big]\\ &\quad - 2\,l\,r\,\cos(\tfrac{\bar\theta_1}{2}-\tfrac{\varphi}{2})\sin(\tfrac{\bar\theta_1}{2}) \;+\; \tfrac12\,r^2\,\sin(\varphi)\\ &\quad\times\big[\bar\theta_1\,\cos\varphi+\big(\ln(\cos(\tfrac{\varphi}{2}))-\ln(\cos(\bar\theta_1+\tfrac{\varphi}{2}))\big)\sin\varphi\big],\end{aligned}\tag{16}$$

$$\begin{aligned}\hat h_0(l,R,r,\varphi) &:= \int_0^{\bar\theta_2} \hat g(l,R,r,\varphi;\theta)\,d\theta\\ &= 2\,l\,R\cos(\tfrac{\bar\theta_2}{2}+\tfrac{\varphi}{2})\,\sin(\tfrac{\bar\theta_2}{2}) - l\,r\big(\sin(\bar\theta_2-\tfrac{\varphi}{2})+\sin\tfrac{\varphi}{2}\big)\\ &\quad - \tfrac12\,R^2\sin(\varphi)\,\big[\bar\theta_2\cos\varphi+\big(\ln(\cos(\bar\theta_2-\tfrac{\varphi}{2}))-\ln(\cos(\tfrac{\varphi}{2}))\big)\sin\varphi\big]\\ &\quad + \tfrac12\,r^2\,\sin(\varphi)\,\big[\bar\theta_2\cos\varphi+\big(\ln(\cos(\tfrac{\varphi}{2}))-\ln(\cos(\bar\theta_2+\tfrac{\varphi}{2}))\big)\sin\varphi\big],\end{aligned}\tag{17}$$

$$\begin{aligned}\bar h_1(l,R,r,\varphi) &:= \int_{\hat\theta_1}^{\bar\theta_1} \bar g(l,r,\varphi;\theta)\,d\theta\\ &= \tfrac18\,l^2\,\csc(\varphi)\big[\,2\,(\bar\theta_1-\hat\theta_1)\cos\varphi+\sin(2\,\bar\theta_1)-\sin(2\,\hat\theta_1)\big]\\ &\quad - 2\,l\,r\cos(\tfrac{\bar\theta_1}{2}+\tfrac{\hat\theta_1}{2}-\tfrac{\varphi}{2})\sin(\tfrac{\bar\theta_1}{2}-\tfrac{\hat\theta_1}{2}) \;+\; \tfrac12\,r^2\sin(\varphi)\\ &\quad\times\big[(\bar\theta_1-\hat\theta_1)\cos\varphi-\big(\ln(\cos(\bar\theta_1+\tfrac{\varphi}{2}))-\ln(\cos(\hat\theta_1+\tfrac{\varphi}{2}))\big)\sin\varphi\big],\end{aligned}\tag{18}$$

$$\begin{aligned}\hat h_1(l,R,r,\varphi) &:= \int_0^{\hat\theta_1} \hat g(l,R,r,\varphi;\theta)\,d\theta\\ &= 2\,l\,R\cos(\tfrac{\hat\theta_1}{2}+\tfrac{\varphi}{2})\,\sin(\tfrac{\hat\theta_1}{2}) - l\,r\big(\sin(\hat\theta_1-\tfrac{\varphi}{2})+\sin\tfrac{\varphi}{2}\big)\\ &\quad - \tfrac12\,R^2\sin(\varphi)\,\big[\hat\theta_1\cos\varphi+\big(\ln(\cos(\hat\theta_1-\tfrac{\varphi}{2}))-\ln(\cos(\tfrac{\varphi}{2}))\big)\sin\varphi\big]\\ &\quad + \tfrac12\,r^2\,\sin(\varphi)\,\big[\hat\theta_1\cos\varphi+\big(\ln(\cos(\tfrac{\varphi}{2}))-\ln(\cos(\hat\theta_1+\tfrac{\varphi}{2}))\big)\sin\varphi\big],\end{aligned}\tag{19}$$

$$\bar{h}_2(l,R,r,\varphi) \;:=\; \int_0^{\hat\theta_2} \bar{g}(l,r,\varphi;\theta)\,d\theta \;=\; \tfrac{1}{8}\,l^2\,\csc(\varphi)\,\big[2\,\hat\theta_2\cos\varphi+\sin(2\,\hat\theta_2)\big] \tag{20}$$
$$-\,2\,l\,r\,\cos(\tfrac{\hat\theta_2}{2}-\tfrac{\varphi}{2})\,\sin(\tfrac{\hat\theta_2}{2})\;+\;\tfrac{1}{2}\,r^2\,\sin(\varphi)$$
$$\times\,\big[\,\hat\theta_2\,\cos\varphi+\big(\ln(\cos(\tfrac{\varphi}{2}))-\ln(\cos(\hat\theta_2+\tfrac{\varphi}{2}))\big)\sin\varphi\big],$$

$$\hat{h}_2(l,R,r,\varphi) \;:=\; \int_{\hat\theta_2}^{\bar\theta_2} \hat{g}(l,R,r,\varphi;\theta)\,d\theta \tag{21}$$
$$=l\,R\,\big[\,\sin(\bar\theta_2+\tfrac{\varphi}{2})-\sin(\hat\theta_2+\tfrac{\varphi}{2})\big]-l\,r\,\big[\,\sin(\bar\theta_2-\tfrac{\varphi}{2})-\sin(\hat\theta_2-\tfrac{\varphi}{2})\big]$$
$$-\,\tfrac{1}{2}\,R^2\sin(\varphi)\,\big[\,(\bar\theta_2-\hat\theta_2)\cos\varphi+\big(\ln(\cos(\bar\theta_2-\tfrac{\varphi}{2}))-\ln(\cos(\hat\theta_2-\tfrac{\varphi}{2}))\big)\sin\varphi\big]$$
$$+\,\tfrac{1}{2}\,r^2\,\sin(\varphi)\,\big[\,(\bar\theta_2-\hat\theta_2)\cos\varphi-\big(\ln(\cos(\bar\theta_2+\tfrac{\varphi}{2}))-\ln(\cos(\hat\theta_2+\tfrac{\varphi}{2}))\big)\sin\varphi\big],$$

$$\hat{h}_{21}(l,R,r,\varphi) \;:=\; \int_{\hat\theta_2}^{\hat\theta_1} \hat{g}(l,R,r,\varphi;\theta)\,d\theta \tag{22}$$
$$=l\,R\,\big[\,\sin(\hat\theta_1+\tfrac{\varphi}{2})-\sin(\hat\theta_2+\tfrac{\varphi}{2})\big]-l\,r\,\big[\,\sin(\hat\theta_1-\tfrac{\varphi}{2})-\sin(\hat\theta_2-\tfrac{\varphi}{2})\big]$$
$$-\,\tfrac{1}{2}\,R^2\sin(\varphi)\,\big[\,(\hat\theta_1-\hat\theta_2)\cos\varphi+\big(\ln(\cos(\hat\theta_1-\tfrac{\varphi}{2}))-\ln(\cos(\hat\theta_2-\tfrac{\varphi}{2}))\big)\sin\varphi\big]$$
$$+\,\tfrac{1}{2}\,r^2\,\sin(\varphi)\,\big[\,(\hat\theta_1-\hat\theta_2)\cos\varphi-\big(\ln(\cos(\hat\theta_1+\tfrac{\varphi}{2}))-\ln(\cos(\hat\theta_2+\tfrac{\varphi}{2}))\big)\sin\varphi\big],$$

Different domains in the diagram of the parameters φ and λ in the Figure 12 show where the h-functions (16) to (22) are defined in particular.

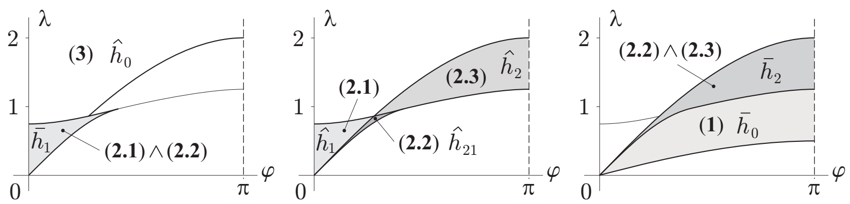

Figure 12: *Case distinctions and domains of h-functions in the φ-λ-diagram*

Proof. All the integrals can immediately derived according to the Lemmata 1 to 5 of Section 2.1.3 and due to the ranges of integration according to Table 2. □

Remark 2. *With respect to the general structure of the h-functions which is*

$$h \;=\; \int_{\theta^{\mathrm{l}}}^{\theta^{\mathrm{u}}} g(\theta)\,d\theta \;=\; \int_{\theta^{\mathrm{l}}}^{\theta^{\mathrm{u}}}\int_{\rho^{\mathrm{l}}}^{\rho^{\mathrm{u}}} f(\theta,\rho)\,d\rho\,\wedge\,d\theta \;=\; \int_{\theta^{\mathrm{l}}}^{\theta^{\mathrm{u}}}\int_{\rho^{\mathrm{l}}}^{\rho^{\mathrm{u}}}\int_{\zeta^{\mathrm{l}}}^{\zeta^{\mathrm{u}}} d\zeta\,\wedge\,d\rho\,\wedge\,d\theta$$

with the above defined functions f and g as subjects of integration and according to their limits in Lemma 6 and the Table 2, respectively, we have access to the following *parts of the measure now:*

$$\begin{aligned}
\bar h_0 &= \mu(T'_{(\mathbf{1}),1}), & \hat h_1 &= \mu(T'_{(\mathbf{2.1}),1}), & \bar h_1 &= \mu(T'_{(\mathbf{2.1}),2}) = \mu(T'_{(\mathbf{2.2}),3}),\\
\hat h_{21} &= \mu(T'_{(\mathbf{2.2}),2}), & \hat h_2 &= \mu(T'_{(\mathbf{2.3}),2}), & \bar h_2 &= \mu(T'_{(\mathbf{2.2}),1}) = \mu(T'_{(\mathbf{2.3}),1}),\\
\hat h_0 &= \mu(T'_{(\mathbf{3}),1}).
\end{aligned}$$

Summarizing all these separated parts as a whole we gain the following main theorem stating the pursued measure $\mu(T)$ in its entirety.

Theorem 1. *The measure of the set T of all segments $\mathcal{S}$ of length $l \geq 0$ intersecting both components of a Kite $\mathcal{K}$ according to definition 1 with an angle $0 \leq \varphi \leq \pi$ is the value of the function*

$$\begin{aligned}
m : \mathbb{R}_0^+ \times \mathbb{R}^+ \times \mathbb{R}_0^+ \times [0,\pi] &\longrightarrow \mathbb{R}_0^+, \\
(l, R, r, \varphi) &\longmapsto \mu(T) =: m(l, R, r, \varphi),
\end{aligned} \tag{23}$$

where m is the sum of case distinctive addends according to **(c)** *in Section 2.2:*

$$m = m_{(\mathbf{c})} = l^2 \cdot U_{(\mathbf{c})} + R^2 \cdot V_{(\mathbf{c})} + r^2 \cdot W_{(\mathbf{c})} + 2\,l\,R \cdot G_{(\mathbf{c})} + 2\,l\,r \cdot H_{(\mathbf{c})},$$

in particular we have $m_{(\mathbf{0})} = 0$ as well as

$$\begin{aligned}
U_{(\mathbf{1})} &= \tfrac12\,[\,\bar\theta_1 \cot\varphi + \tfrac12\,], & G_{(\mathbf{1})} &= 0,\\
U_{(\mathbf{2.1})} &= \tfrac12\,[(\bar\theta_1 - \hat\theta_1)\cot\varphi + 1\,], & G_{(\mathbf{2.1})} &= \tfrac34\cos(\varphi)\cdot\Psi(\tfrac{R}{l}) - \sin\tfrac{\varphi}{2},\\
U_{(\mathbf{2.2})} &= \tfrac12\,[(\bar\theta_1 + \hat\theta_2 - \hat\theta_1)\cot\varphi + \tfrac12\,], & G_{(\mathbf{2.2})} &= \tfrac32\cos(\varphi)\cdot\Psi(\tfrac{R}{l}),\\
U_{(\mathbf{2.3})} &= \tfrac12\,[\,\hat\theta_2 \cot\varphi - \tfrac12\,], & G_{(\mathbf{2.3})} &= \tfrac34\cos(\varphi)\cdot\Psi(\tfrac{R}{l}) + \Psi(\tfrac{r}{d}),\\
U_{(\mathbf{3})} &= 0, & G_{(\mathbf{3})} &= \Psi(\tfrac{r}{d}) - \sin\tfrac{\varphi}{2}
\end{aligned}$$

and

$$\begin{aligned}
V_{(\mathbf{1})} &= 0,\\
V_{(\mathbf{2.1})} &= \sin(\varphi)\cdot\big[\quad - \hat\theta_1\,\cos\varphi + \big(\tfrac32 - \ln(\tfrac{a}{l})\big)\sin\varphi\big],\\
V_{(\mathbf{2.2})} &= \sin(\varphi)\cdot\big[(\hat\theta_2 - \hat\theta_1)\cos\varphi\big],\\
V_{(\mathbf{2.3})} &= \sin(\varphi)\cdot\big[(\hat\theta_2 - \bar\theta_2)\cos\varphi - \big(\tfrac32 + \ln(\tfrac{l}{d})\big)\sin\varphi\big],\\
V_{(\mathbf{3})} &= \sin(\varphi)\cdot\big[\quad - \bar\theta_2\,\cos\varphi - \ln(\tfrac{a}{d})\sin\varphi\big]
\end{aligned}$$

as well as

$$\begin{aligned}
W_{(\mathbf{1})} = W_{(\mathbf{2.1})} = W_{(\mathbf{2.2})} &= \sin(\varphi)\cdot\big[\bar\theta_1\cdot\cos\varphi + \big(\tfrac32 - \ln(\tfrac{b}{l})\big)\sin\varphi\big]\\
W_{(\mathbf{2.3})} = W_{(\mathbf{3})} &= \sin(\varphi)\cdot\big[\bar\theta_2\cdot\cos\varphi - \ln(\tfrac{b}{d})\sin\varphi\big]
\end{aligned}$$

and

$$H_{(\mathbf{1})} = H_{(\mathbf{2.1})} = H_{(\mathbf{2.2})} = -\tfrac{3}{4}\cos(\varphi)\cdot\Psi(\tfrac{r}{l}) - \sin\tfrac{\varphi}{2}$$
$$H_{(\mathbf{2.3})} = H_{(\mathbf{3})} = -\cos(\varphi)\cdot\Psi(\tfrac{r}{d}) + \tfrac{r}{d}\sin^2\varphi - \sin\tfrac{\varphi}{2}$$

with

$$\Psi(\psi) \;=\; \sqrt{1-\psi^2\cdot\sin^2\varphi}$$

including the following quantities consisting of R, r, and φ, see also Table 1,

$$a \;=\; 2\,R\sin\tfrac{\varphi}{2}\,,\;\; b \;=\; 2\,r\sin\tfrac{\varphi}{2}\,,\;\; d \;=\; \sqrt{R^2+r^2-2\,R\,r\cos\varphi}\,,$$

and the angles $\hat{\theta}_1$ and $\hat{\theta}_2$ according to (10) and (11) as well as $\bar{\theta}_1$ and $\bar{\theta}_2$ according to (12) and (13).

Proof. Since the subsets $T'_{(\mathbf{c}),i}$ with $i = 1,...,n_{(\mathbf{c})}$ in (15) are disjoint we gain the case distinctive measures in form of the sum

$$\mu(T'_{(\mathbf{c})}) \;=\; \sum_{i=1}^{n_{(\mathbf{c})}} \mu(T'_{(\mathbf{c}),i}) \;=\; \sum_{i=1}^{n_{(\mathbf{c})}} \int_{b^{\mathrm{l}}_{(\mathbf{c}),i}}^{b^{\mathrm{u}}_{(\mathbf{c}),i}} dS \qquad (*)$$

and further according to Section 2.1.2 in usage of the axial symmetry we have eventually $\mu(T_{(\mathbf{c})}) \;=\; 2\cdot\mu(T'_{(\mathbf{c})})$. Due to (3) the integrals in the sum (*) are of the form

$$\mu(T'_{(\mathbf{c}),i}) \;=\; \int_{b^{\mathrm{l}}_{(\mathbf{c}),i}}^{b^{\mathrm{u}}_{(\mathbf{c}),i}} dS \;=\; \int_{\theta^{\mathrm{l}}_{(\mathbf{c}),i}}^{\theta^{\mathrm{u}}_{(\mathbf{c}),i}} \int_{\rho^{\mathrm{l}}_{(\mathbf{c}),i}}^{\rho^{\mathrm{u}}_{(\mathbf{c}),i}} \int_{\zeta^{\mathrm{l}}_{(\mathbf{c}),i}}^{\zeta^{\mathrm{u}}_{(\mathbf{c}),i}} d\zeta\wedge d\rho\wedge d\theta\,. \qquad (**)$$

According to the limits of integration in Table 2 and the Lemma and Definition 6 respectively with the h-functions and their meaning for the measures of the subsets $\mu(T'_{(\mathbf{c}),i})$ we have with respect to the sum (*) and the addends (**) now

$$\mu(T_{(\mathbf{1})}) = 2\cdot\bar{h}_0$$
$$\mu(T_{(\mathbf{2.1})}) = 2\cdot(\hat{h}_1+\bar{h}_1) \qquad \mu(T_{(\mathbf{2.2})}) = 2\cdot(\bar{h}_2+\hat{h}_{21}+\bar{h}_1)$$
$$\mu(T_{(\mathbf{2.3})}) = 2\cdot(\bar{h}_2+\hat{h}_2) \qquad \mu(T_{(\mathbf{3})}) = 2\cdot\hat{h}_0.$$

Substituting all the h-functions from (16) to (22) and simplifying the expressions we get the case distinctive measure in form of the function m in (23). □

Remark 3. *The case distinctive relations $m_{(\mathbf{c})}$ of the measure $\mu(T)$ are equal to each other at the boundaries of the domains: $l = b$: $(\mathbf{0})$=$(\mathbf{1})$, $l = p$: $(\mathbf{1})$=$(\mathbf{2.2})$ for $0\le\varphi\le\bar{\varphi}$, $l = d$: $(\mathbf{1})$=$(\mathbf{2.3})$ for $\bar{\varphi}\le\varphi\le\pi$, $l = a$: $(\mathbf{2.1})$=$(\mathbf{2.2})$ for $0\le\varphi\le\hat{\varphi}$, $l = d$: $(\mathbf{2.2})$=$(\mathbf{2.3})$ for $\hat{\varphi}\le\varphi\le\bar{\varphi}$, $l = d$: $(\mathbf{2.1})$=$(\mathbf{3})$ for $0\le\varphi\le\hat{\varphi}$ and $l = a$: $(\mathbf{2.3})$=$(\mathbf{3})$ for $\hat{\varphi}\le\varphi\le\pi$. Additionally, all measures are once continuous differentiable at the boundaries.*

Remark 4. *In the case of $\varphi\to 0$ the measure $\mu(T)$ is the same as the classical one for the intersection of two segments. Here the valid cases are $(\mathbf{2.1})$ and $(\mathbf{3})$ which correspond in $\lim_{\varphi\to 0} m_{(\mathbf{2.1})}(l,R,r,\varphi) = \lim_{\varphi\to 0} m_{(\mathbf{3})}(l,R,r,\varphi) = 2(R-r)l$. For a straight angle φ the measure of all segments $\mathcal{S}$ with two intersections to the Kite vanishes since all segments $\mathcal{S}$ are collinear to $\mathcal{K}_1$ and $\mathcal{K}_2$ of the Kite: $\lim_{\varphi\to\pi} m_{(\mathbf{1})}(l,R,r,\varphi) = \lim_{\varphi\to\pi} m_{(\mathbf{2.3})}(l,R,r,\varphi) = \lim_{\varphi\to\pi} m_{(\mathbf{3})}(l,R,r,\varphi) = 0$.*

4. Outlook

Now we are able to show that it is only once necessary to integrate in such costly way we carried out above to answer the following general question by using Theorem 1 and the principle of inclusion – exclusion (PIE in short). Suppose a pair of fixed segments $\mathcal{A} := \mathcal{A}_1 \cup \mathcal{A}_2$ in the plane, then: What is the measure of all segments $\mathcal{S}$ of constant length that intersect both of them, i.e. $\mathcal{A}_1$ and $\mathcal{A}_2$?

We can reduce this question to the pairs of segments according to Table 3 and Figure 13. How to "reach" all this pairs of two segments starting with the measure of the Kite? Figure 13 reveals, that in the beginning two limits are sufficient to form the Angle and the Rectangle out of the Kite; afterwards only a combination of this figures are necessary to gain all the other ones and their sets and measures respectively.

Name	Fixed Pair $\mathcal{A}$	Set $A = \{\mathcal{S} \mid \#(\mathcal{A} \cap \mathcal{S}) = 2\}$
Kite	$\mathcal{K}(R, r, \varphi)$	$T = T(l, R, r, \varphi)$
Rectangle	$\mathcal{R}(t, a)$	$B = B(l, t, a)$
Trapezium	$\mathcal{T}(u, v, a)$	$D = D(l, u, v, a)$
Parallel	$\mathcal{P}(s_1, s_2, t, a)$	$U = U(l, s_1, s_2, t, a)$
Angle	$\mathcal{V}(R, \varphi)$	$V = V(l, R, \varphi) = T(l, R, 0, \varphi)$
Cross	$\mathcal{C}(R, r, \varphi)$	$C = C(l, R, r, \varphi)$
Hook	$\mathcal{H}(R, r, \varphi)$	$H = H(l, R, r, \varphi)$
Transverse	$\mathcal{Q}(R_1, r_1, R_2, r_2, \varphi)$	$Q = Q(l, R_1, r_1, R_2, r_2, \varphi)$

Table 3: *Pairs of fixed segments and sets of moveable segments intersecting both of them*

We start with the upper part of Figure 13: The measure of the set V for segments hitting an Angle $\mathcal{V}$ twice is simply a result of $r \to 0$. The next figure of interest is the Hook $\mathcal{H}$ reachable by the detour of an upper and lower Cross $\mathcal{C}$.

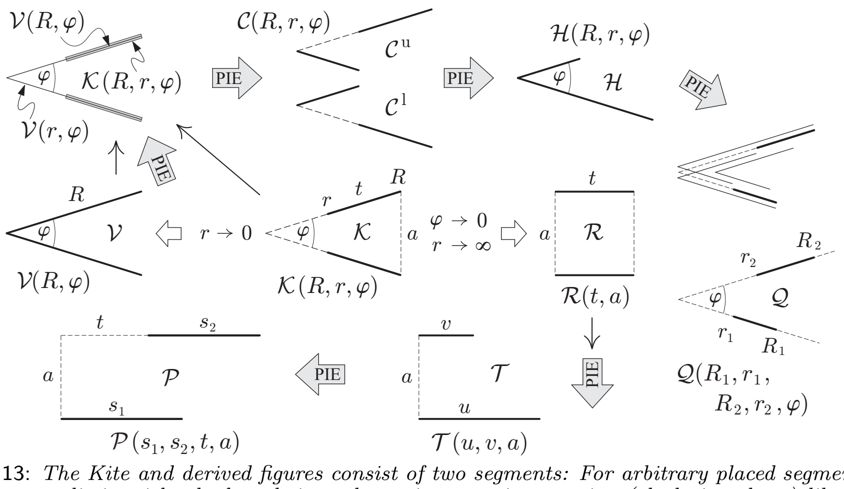

Figure 13: *The Kite and derived figures consist of two segments: For arbitrary placed segments we have just to distinguish whether their prolongations are intersecting (clockwise above) like figure $\mathcal{Q}$ or whether they are parallel (anticlockwise below) like figure $\mathcal{P}$*

Here we have with the union of disjoint sets (see Figure 13 on the upper line, far left)

$$V(l,R,\varphi) \,=\, V(l,r,\varphi) \,\cup\, C^{\mathrm{u}}(l,R,r,\varphi) \,\cup\, C^{\mathrm{l}}(l,R,r,\varphi) \,\cup\, T(l,R,r,\varphi)\,.$$

Since there is as well $\mu(C^{\mathrm{u}}(l,R,r,\varphi)) = \mu(C^{\mathrm{l}}(l,R,r,\varphi)) =: \mu(C(l,R,r,\varphi))$ we gain the first new result

$$\mu\big(C(l,R,r,\varphi)\big) \,=\, \tfrac{1}{2}\cdot\big[\,\mu\big(V(l,R,\varphi)\big) \,-\, \mu\big(V(l,r,\varphi)\big) \,-\, \mu\big(T(l,R,r,\varphi)\big)\big] \tag{24}$$

for a Cross $\mathcal{C}$; note that the measure is independent of the orientation of the Cross! In other words the union of the Crosses is equal to the difference of a small and a large Angle and of an appropriate Kite:

$$C^{\mathrm{u}}(l,R,r,\varphi) \,\cup\, C^{\mathrm{l}}(l,R,r,\varphi) \,=\, V(l,R,\varphi)\setminus\big(V(l,r,\varphi)\cup T(l,R,r,\varphi)\big).$$

Now the set of segments $\mathcal{S}$ intersecting both sides of a Hook $\mathcal{H}$ (radiuses r and R) is the union of a small Angle (radius r) and a matching Cross, i.e.

$$H(l,R,r,\varphi) \,=\, V(l,r,\varphi) \,\cup\, C^{\mathrm{l}}(l,R,r,\varphi).$$

With respect to the construction of the pairs of segments once more all this sets are disjointed[§]. With the appelation and the result (24) we reach to

$$\mu\big(H(l,R,r,\varphi)\big) \,=\, \tfrac{1}{2}\cdot\big[\,\mu\big(V(l,R,\varphi)\big) \,+\, \mu\big(V(l,r,\varphi)\big) \,-\, \mu\big(T(l,R,r,\varphi)\big)\big]. \tag{25}$$

The sets for Hooks have to combine in an adroit way, see right part of Figure 13:

$$H(l,R_1,R_2,\varphi) \,=\, H(l,R_1,r_2,\varphi) \,\cup\, H(l,r_1,R_2,\varphi) \,\cup\, Q(l,R_1,r_1,R_2,r_2,\varphi)$$

here with $H(l,R_1,r_2,\varphi)\cap H(l,r_1,R_2,\varphi) \,=\, H(l,r_1,r_2,\varphi)$ while once more all the other sets are disjointed. So the PIE delivers for the general Traverse $\mathcal{Q}$ the result

$$\begin{aligned}\mu\big(Q(l,R_1,r_1,R_2,r_2,\varphi)\big) &= \mu\big(H(l,R_1,R_2,\varphi)\big) \,+\, \mu\big(H(l,r_1,r_2,\varphi)\big)\\ &\quad -\mu\big(H(l,R_1,r_2,\varphi)\big) \,-\, \mu\big(H(l,r_1,R_2,\varphi)\big)\\ &= \tfrac{1}{2}\cdot\big[\,\mu\big(T(l,R_1,r_2,\varphi)\big) \,+\, \mu\big(T(l,r_1,R_2,\varphi)\big)\\ &\quad -\mu\big(T(l,R_1,R_2,\varphi)\big) \,-\, \mu\big(T(l,r_1,r_2,\varphi)\big)\big]\end{aligned} \tag{26}$$

using the measures of four Hooks or as well as of four Kites; note, avoiding an awkward notation using $\max(R_1,R_2)$ and $\max(r_1,r_2)$ and so on, the order of arguments of the radiuses depends on the relations $R_1 \lesseqgtr R_2$, $r_1 \lesseqgtr r_2$, $R_1 \lesseqgtr r_2$, and $r_1 \lesseqgtr R_2$.

Similarly we conquer two parallel arbitrary placed segments, a so called Parallel $\mathcal{P}$, starting with a Rectangle $\mathcal{R}$ and a Trapezium $\mathcal{T}$. According to Figure 14 we have the disjoint sets $B = B_{\mathrm{l}}\cup B_{\mathrm{r}}\cup Z_{\mathrm{lr}}\cup Z_{\mathrm{rl}}$ where B, B_{l}, and B_{r} are the sets of segments $\mathcal{S}$ hitting the depicted Rectangles $\mathcal{R}$, $\mathcal{R}_{\mathrm{l}}$, and $\mathcal{R}_{\mathrm{r}}$ respectively as well as Z_{lr} and Z_{rl} which are the analogous sets for the "$\mathcal{Z}$-figures". Due to $\mu(Z_{\mathrm{lr}}) = \mu(Z_{\mathrm{rl}}) =: \mu(Z)$ this union of sets delivers $\mu(Z) = \frac{1}{2}[\mu(B)-\mu(B_{\mathrm{l}})-\mu(B_{\mathrm{r}})]$. Thus for the set $D = B_{\mathrm{l}}\cup Z_{\mathrm{lr}}$

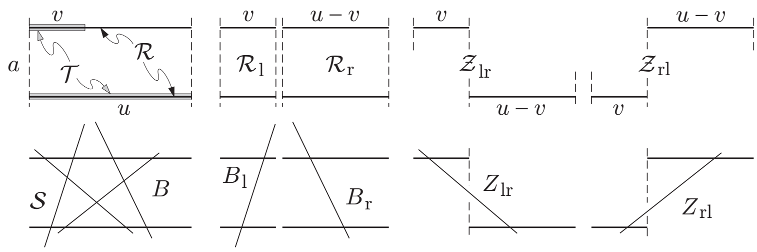

Figure 14: *Journey from a Rectangle $\mathcal{R}$ to a Trapezium $\mathcal{T}$, see also Figure 13*

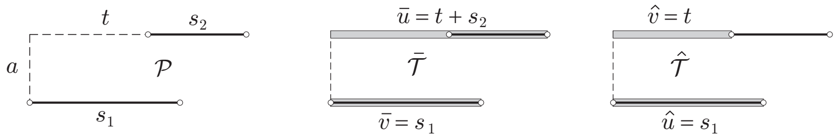

Figure 15: *A Parallel $\mathcal{P}$ formed by two Trapezium $\bar{\mathcal{T}}$ and $\hat{\mathcal{T}}$*

of all segments crossing the Trapezium $\mathcal{T}$ it turns out that $\mu(D) = \mu(B_l) + \mu(Z_{lr})$, so we have

$$\mu\big(D(l,u,v,a)\big) \;=\; \tfrac{1}{2}\cdot\big[\mu\big(B(l,u,a)\big) \;+\; \mu\big(B(l,v,a)\big) - \mu\big(B(l,u-v,a)\big)\big].$$

To contribute the last part in this map of pairs of segments we look at Figure 15. Beginning at the left edge of the Parallel $\mathcal{P}$ we place two Trapezium $\bar{\mathcal{T}}$ and $\hat{\mathcal{T}}$ along the Parallel, so for the sets of segments $\mathcal{S}$ that intersect both components of each pair we have $U \cup \hat{D} = \bar{D}$ with $U \cap \hat{D} = \emptyset$. Hence $\mu(U) = \mu(\bar{D}) - \mu(\hat{D})$ that becomes

$$\mu\big(U(l,s_1,s_2,t,a)\big) \;=\; \mu\big(D(l,t+s_2,s_1,a)\big) - \mu\big(D(l,s_1,t,a)\big)$$

written in appropriate arguments. – If the two arbitrary placed segments $\mathcal{A}_1$ and $\mathcal{A}_2$ occur in such a way which is depicted in Figure 16, it will be possible to partition them into figures we have just discussed. Due to the fact that this is in all cases in a disjointed way possible, there are no new figures, sets or measures necessary.

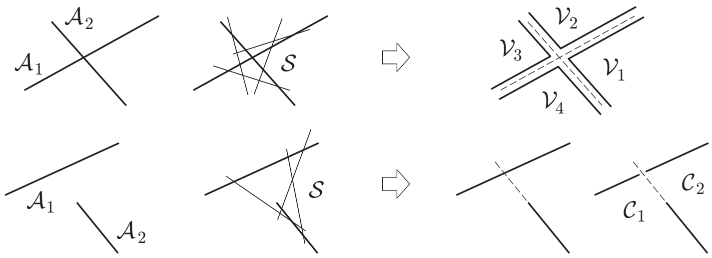

Figure 16: *Figures $\mathcal{A}_1 \cup \mathcal{A}_2$ which can be reduced into already known basis figures*

Finally, if we have the measure $\mu(A^2)$ of the set $A^2 := \{\mathcal{S} \,|\, \#(\mathcal{S} \cap \mathcal{A}) = 2\}$ for a pair $\mathcal{A} = \mathcal{A}_1 \cup \mathcal{A}_2$ of segments $\mathcal{A}_1$ and $\mathcal{A}_2$ with lengths L_1 and L_2 respectively it

§To reduce the technical effort, we avoid to scrutinize for subsets of segments lying collinear to one side of a two sides element, since such sets are of zero measure.

will not be difficult to calculate the measure $\mu(A^1)$, i.e. for the set

$$A^1 := \{\mathcal{S} \mid \#(\mathcal{S} \cap \mathcal{A}) = 1\} = \{\mathcal{N} \mid \mathcal{S} \cap \mathcal{A}_1 \neq \emptyset \not\leftrightarrow \mathcal{S} \cap \mathcal{A}_2 \neq \emptyset\}$$

of all segments $\mathcal{S}$ that intersect the figure $\mathcal{A}$ exactly once. Let $\tilde{A}$ be the set of all segments $\mathcal{S}$ of length l hitting the pair $\mathcal{A}$ at all, that is

$$\tilde{A} := \{\mathcal{S} \mid \#(\mathcal{S} \cap \mathcal{A}) > 0\} = \{\mathcal{N} \mid \mathcal{S} \cap \mathcal{A}_1 \neq \emptyset \vee \mathcal{S} \cap \mathcal{A}_2 \neq \emptyset\}$$

and $A_i := \{\mathcal{S} \mid \mathcal{S} \cap \mathcal{A}_i \neq \emptyset\}$, $i = 1, 2$, the sets of segments hitting the segments $\mathcal{A}_i$. So we have

$$\tilde{A} = A^1 \cup A^2 = A_1 \cup A_2$$

and according to the PIE with $A^1 \cap A^2 = \emptyset$ and $A_1 \cap A_2 = A^2$ we gain the equation

$$\begin{aligned}\mu(\tilde{A}) &= \mu(A^1) + \mu(A^2) - \mu(A^1 \cap A^2) = \mu(A^1) + \mu(A^2)\\ &= \mu(A_1) + \mu(A_2) - \mu(A_1 \cap A_2) = \mu(A_1) + \mu(A_2) - \mu(A^2)\end{aligned}$$

and with $\mu(A_i) = 2lL_i$, see [6], we have

$$\mu(A^1) = 2 \cdot \left[lL - \mu(A^2)\right] \tag{27}$$

with $L := L_1 + L_2$ as the total length of the pair of segments $\mathcal{A}$. Hence we demonstrated how important it is to have the knowledge of the measure $\mu(A^2)$. In fact it is possible to derive even the measure $\mu(A^1)$ directly, but generally it is much more difficult to cope with one segment all the time as an obstacle, which must not be hit by the moveable segment. And due to reasons of symmetry it is much more convenient to work with the pair of both segments. – Thus, the objective is reached to reduce the measure of all segments intersecting a pair of segments twice to the measure for the Kite.

5. Applications in probabilities

1. The measures above can be used in a variety of applications to calculate geometric probabilities. For the beginning we like to know: What is the geometric probability that a randomly placed segment $\mathcal{S}$ hitting a Kite $\mathcal{K}$ does that in such a way that both segments $\mathcal{K}_1$ and $\mathcal{K}_2$ are matched?

Theorem 2. *Let $\mathcal{K}$ be a Kite with segments of length $R - r > 0$ according to Definition 1. For randomly placed segments $\mathcal{S}$ of length $l \geq 0$ in the plane we have the conditional probability*

$$\begin{aligned}p(\#(\mathcal{S} \cap \mathcal{K}) = 2 \mid \mathcal{S} \cap \mathcal{K} \neq \emptyset) &= \frac{\mu(T)}{4l(R-r) - \mu(T)}\\ &= \frac{l^2 U_{(\mathbf{f})} + R^2 V_{(\mathbf{f})} + r^2 W_{(\mathbf{f})} + 2lRG_{(\mathbf{f})} + 2lrH_{(\mathbf{f})}}{4l(R-r) - l^2 U_{(\mathbf{f})} - R^2 V_{(\mathbf{f})} - r^2 W_{(\mathbf{f})} - 2lRG_{(\mathbf{f})} - 2lrH_{(\mathbf{f})}}\end{aligned}$$

for a match of both segments $\mathcal{K}_1$ and $\mathcal{K}_2$ of the Kite for all segments $\mathcal{S}$ in the plane hitting the Kite in general. We have $\mu(T)$ and $U_{(\mathbf{f})}$, $V_{(\mathbf{f})}$, $W_{(\mathbf{f})}$ as well as $G_{(\mathbf{f})}$ and $H_{(\mathbf{f})}$ according to Theorem 1.

Proof. With $K = \{\mathcal{S} \mid \mathcal{S} \cap \mathcal{K} \neq \emptyset\}$ and once more $T = \{\mathcal{S} \mid \#(\mathcal{S} \cap \mathcal{K}) = 2\}$ we have due to the relation $T \subset K$ the probability

$$p(T \mid K) \;=\; \frac{p(T \cap K)}{p(K)} \;=\; \frac{p(T)}{p(K)} \;=\; \frac{\mu(T)}{\mu(K)}\,.$$

If we introduce the sets $K_i := \{\mathcal{S} \mid \mathcal{S} \cap \mathcal{K}_i \neq \emptyset\}$, $i = 1, 2$, for all segments $\mathcal{S}$ hitting the side $\mathcal{K}_i$ of the Kite $\mathcal{K}$ we have according to $\mu(K_1) = \mu(K_2) = 2l(R-r)$, see [6], p.89f, and $\mu(K_1 \cap K_2) = \mu(T)$ the measure

$$\mu(K) \;=\; \mu(K_1 \cup K_2) \;=\; \mu(K_1) + \mu(K_2) - \mu(K_1 \cap K_2) \;=\; 2 \cdot 2l\,(R-r) - \mu(T)$$

and therefore $p(T \mid K) = \mu(T)/\mu(K) = \mu(T)/(4l\,(R-r) - \mu(T))$. $\square$

The diagram in Figure 17 shows the conditional probability $p(T \mid K)$ in dependence of the length l of the segment $\mathcal{S}$ and the angle φ of the Kite $\mathcal{K}$. We have $p(T \mid K) = 1$ for $\varphi = 0$ and $p(T \mid K) = 0$ for $\varphi = \pi$.

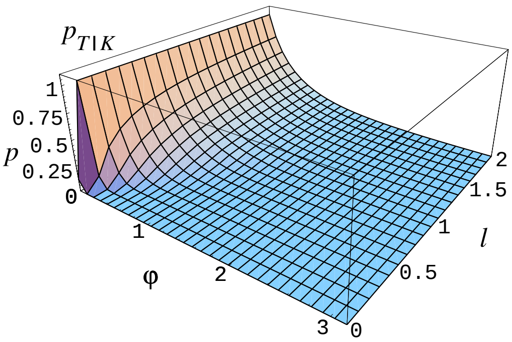

Figure 17: *Geometric Probability $p(T \mid K)$ according to Theorem 2 for $R = 1$ and $r = \frac{1}{3}$*

Monte Carlo Tests

For all the discussed geometric configuration we achieved large quantities of simulations. Some extract of this results will be presented here in a form of an overview.

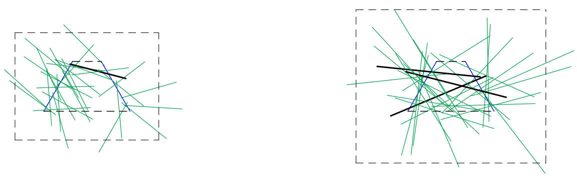

Figure 18: *Monte Carlo Test with a Kite inside a rectangle, segments $\mathcal{S}$ are uniformly distributed on the rectangle, segments without a match of the Kite are removed, here: 30 segments $\mathcal{S}$ a time are hitting the Kites*

Figure 18 shows two Monte Carlo Tests of 30 segments a time on Kites with $R = 1$, $r = \frac{1}{3}$, and $\varphi = 60°$. On the left $l = \frac{2}{3}$, thus the measure $\mu(T)$ is of case (**1**), and on the right we have segments of length $l = \frac{6}{5}$, hence $\mu(T)$ is according to case (**3**). The centres of the segments are uniformly distributed inside the rectangle (broken line in the figure). Only segments are considered hitting at least one side of the Kite. Segments cutting both sides of the Kites are emphasized in bold lines. In the next Figure 19 we evaluated relative frequencies up to 1000 segments of different lengths according to the depicted cases in the centre of the figure. The consecutively calculated averages of the numbers of two-cuts are shown in form of trends which can be compared to the analytical values in form of horizontal lines.

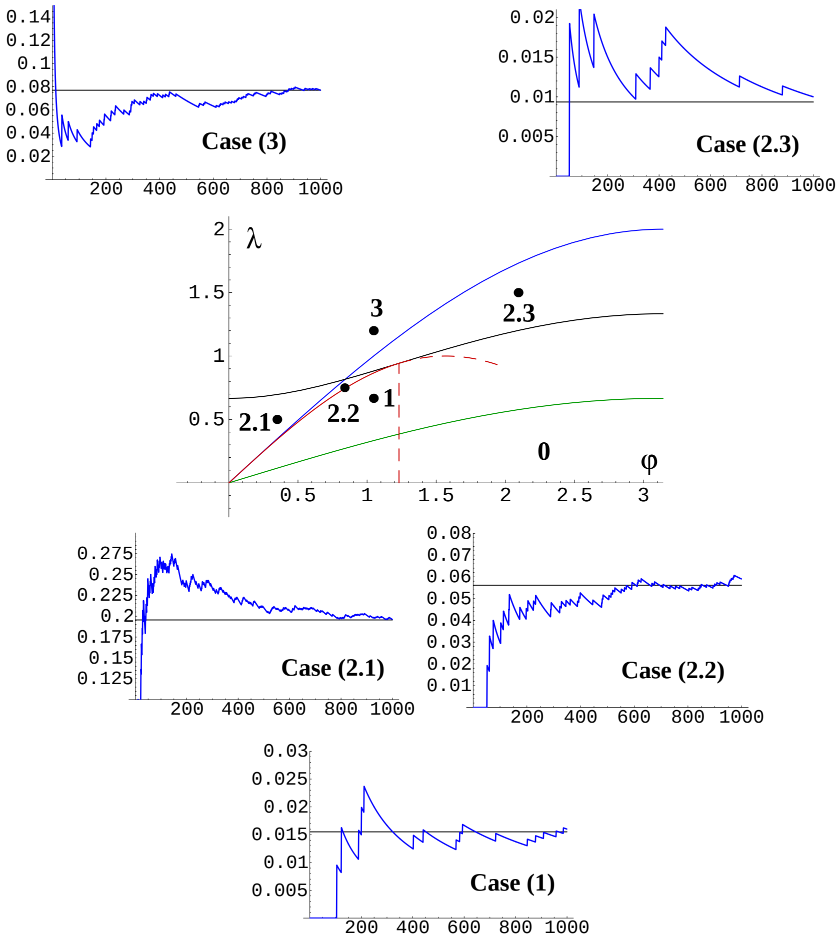

Figure 19: *Relative frequencies for double matches; compare the diagram of parameters in the centre: clockwise beginning above on the left, evaluations according to Cases (3), (2.3), (1), (2.2), and (2.1)*

2. In a similar manner we now ask: What is the geometric probability that a randomly placed segment $\mathcal{S}$ on the convex hull of a Kite $\mathcal{K}$ will hit both segments

$\mathcal{K}_1$ and $\mathcal{K}_2$ of the Kite?

Theorem 3. *Let $\mathcal{K}$ be a Kite with segments of length $R - r > 0$ according to Definition 1. For randomly placed segments $\mathcal{S}$ of length $l \geq 0$ in the plane we have the conditional probability*

$$p(\#(\mathcal{S} \cap \mathcal{K}) = 2 \,|\, \mathcal{S} \cap C \neq \emptyset) = \frac{\lambda^2 U_{(\mathbf{f})} + V_{(\mathbf{f})} + \eta^2 W_{(\mathbf{f})} + 2\lambda G_{(\mathbf{f})} + 2\lambda\eta H_{(\mathbf{f})}}{2\,\lambda(1+\eta)\sin\frac{\varphi}{2} + (1-\eta)(2\,\lambda + \frac{\pi}{2}\,(1+\eta)\sin\varphi)}$$

for a match of both sides $\mathcal{K}_1$ and $\mathcal{K}_2$ of the Kite for all segments $\mathcal{S}$ in the plane hitting the convex hull C of the Kite. We have $U_{(\mathbf{f})}$, $V_{(\mathbf{f})}$, $W_{(\mathbf{f})}$ as well as $G_{(\mathbf{f})}$ and $H_{(\mathbf{f})}$ according to Theorem 1.

Proof. Let $A := \{\mathcal{S} \,|\, C \cap \mathcal{S} \neq \emptyset\}$ be the set of all segments in the plane which have at least one point in common with the convex hull C of the Kite $\mathcal{K}$. Once more let $T = \{\mathcal{S} \,|\, \#(\mathcal{S} \cap \mathcal{K}) = 2\}$ the set of segments in the plane cutting the Kite two times. Due to the relation $T \subset A$ we derive the conditional probability

$$p(T \,|\, A) \;=\; \frac{p(T \cap A)}{p(A)} \;=\; \frac{p(T)}{p(A)} \;=\; \frac{\mu(T)}{\mu(A)}. \qquad (*)$$

According to [6] we have the measure

$$\mu(A) \;=\; \pi\,F + l\,U \;=\; 2l(R+r)\sin\tfrac{\varphi}{2} + (R-r)(2l + \tfrac{\pi}{2}\,(R+r)\sin\varphi)$$

with $F = \frac{a+b}{2} \cdot t\cos\frac{\varphi}{2}$ for the area and $U = a + b + 2t$ for the perimeter of the konvex hull C, the meaning and formulas of a, b, t, and φ respectively are displayed in Table 1. In usage of the parameters λ and η, once more according to table 1, we calculate for (*) the expression in the theorem taking only relative parameters! □

Monte Carlo Tests

Now we have to detect segments uniformly distributed inside the rectangle with at least one point in common of the convex hull which is a trapezium. Figure 20 shows simulations with 30 segments $\mathcal{S}$ a time are hitting the convex hulls of the depicted Kites with $R = 1$, $r = \frac{1}{3}$, and $\varphi = 60°$; on the left we have segments of length $l = \frac{2}{3}$ (case (**1**)), on the right we have $l = \frac{6}{5}$ (case (**3**)).

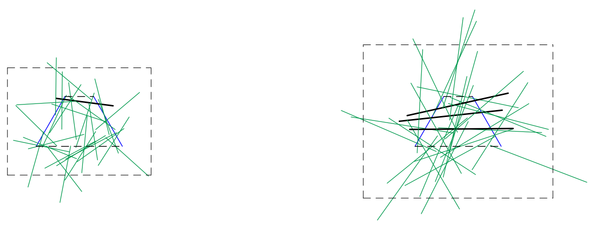

Figure 20: *Monte Carlo Test: segments on the convex hull of the Kite inside a rectangle*

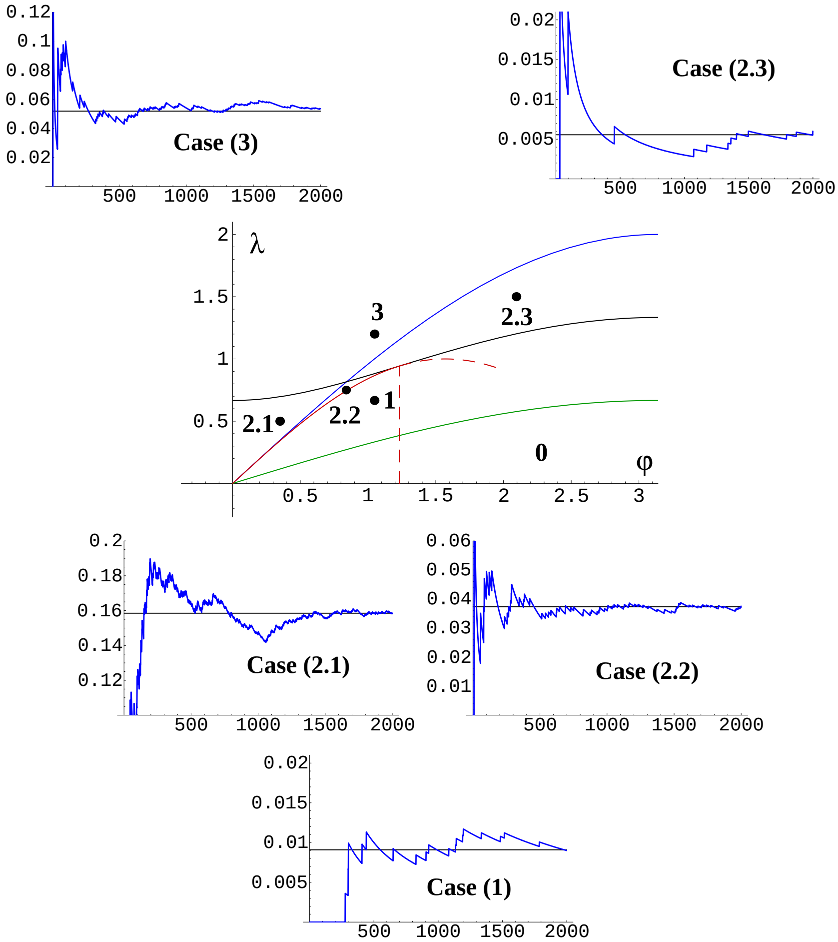

Figure 21: *Relative frequencies for double matches according to the depicted cases*

Figure 21 shows evaluations of relative frequencies up to 2000 segments on the convex hull for the different cases, i.e. length $l = \frac{2}{3}$ for case **(1)**, $l = \frac{1}{2}$ for case **(2.1)**, $l = \frac{3}{4}$ for case **(2.2)**, $l = \frac{3}{2}$ for case **(2.3)**, and $l = \frac{6}{5}$ for case **(3)**. The consecutively calculated averages of the numbers of two-cuts are shown as trends which can be compared to the analytical values in form of horizontal lines.

Considerations of the expected value for the number of intersections

Now we define the following random variable counting the numbers of intersections between movable segments $\mathcal{S}$ in the plane, which are gathered by some definition in a set S of events, and an arbitrary two-segment-element $\mathcal{A}$:

$$X : S \longrightarrow \{0, 1, 2\} = \mathbb{N}_{0,2}\,,\ \mathcal{S} \longmapsto \#(\mathcal{S} \cap \mathcal{A}).$$

With $S_k := \{\mathcal{S} \,|\, \#(\mathcal{S} \cap \mathcal{A}) = k\}$, $k \in \mathbb{N}_{0,2}$, for the sets of segments $\mathcal{S} \in S$ with a

k-fold intersection we have

$$p_k = \frac{\mu(S_k)}{\mu(S)}$$

for the geometric probability of the event of a k-fold intersection between $\mathcal{S}$ and $\mathcal{A}$. These geometric probabilities form the mass function of the random variable X. To go more into detail we have

$$S = S_0 \cup S_1 \cup S_2 \text{ with disjoint sets, so that } S_0 = S \backslash (S_1 \cup S_2)\,.$$

Hence using the formula (27) for $\mu(S_1)$ we receive the probabilities

$$p_0 = \frac{\mu(S_0)}{\mu(S)} = 1 - p_1 - p_2\,,\ \ p_1 = \frac{\mu(S_1)}{\mu(S)} = \frac{2\,l\,L - 2\,\mu(S_2)}{\mu(S)}\,,\ \ p_2 = \frac{\mu(S_2)}{\mu(S)}\,,$$

with L for the total length of the element $\mathcal{A}$ and l for the length of the segment $\mathcal{S}$. The expected value for the number of intersections becomes

$$E(X) = \sum_{k=0}^{2} k \cdot p_k = p_1 + 2p_2 = \frac{2\,l\,L}{\mu(S)}\,.$$

This is a remarkable result: The mean number of intersections does not depend on the measures $\mu(S_1)$ or $\mu(S_2)$ and hence is independent of the case distinctions. We met already such a situation in [3] – and this sort of random experiment is once more of the type of a sequential lattice, which were introduced and examined in that paper.

According to our last scenario of segments placed randomly on the convex hull of a Kite we have

$$E(X) = \frac{2\,(1-\eta)\,\lambda}{(1+\eta)\,\lambda\sin\frac{\varphi}{2} + (1-\eta)\,(\lambda + \frac{\pi}{4}\,(1+\eta)\sin\varphi)}$$

with the parameters λ and η according to Table 1.

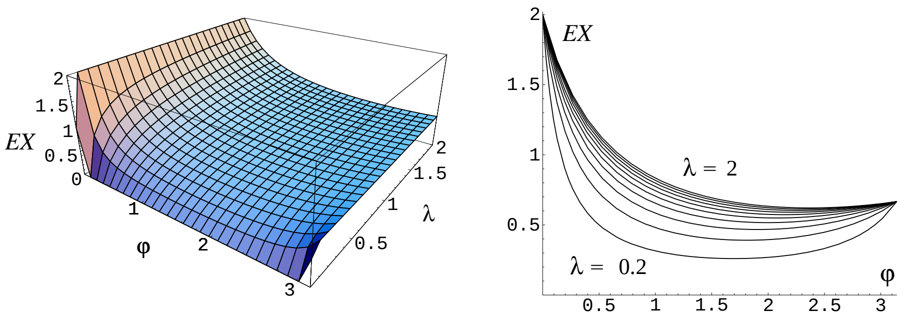

Figure 22: *On the left:* $E(X)$ *for* $\eta = \frac{1}{3}$ *as a function of the angle* φ *and the paramter* $\lambda = \frac{l}{R}$*, on the right: curves of* λ*-cuts in steps of 0.2*

Figure 22 shows this function for $\eta = \frac{1}{3}$ in dependency of φ and λ. Interestingly there are some pronounced minima to see! Hence we can find for each $\lambda = \frac{l}{R}$, i.e.

for each length l of a segement while the sides R, r, and the angle φ are given due to the Kite, minimizing the mean number of cuts for randomly placed segments on the convex hull of the Kite.

In general we have for the boundary on the right hand side at an angle of $\varphi = \pi$ the value $E(X) = 1 - \eta$ and on the left hand side at $\varphi = 0$ the value $E(X) = 2$, since both of the sides of the Kite are matching in one and the same segment – and the convex hull is this only remaining segment itself.

References

[1] R. Böttcher,, *Geometrische Wahrscheinlichkeiten vom Buffonschen Typ in begrenzten Gittern*, FernUniversität in Hagen, 2005, available at `http://deposit.fernuni-hagen.de/volltexte/2006/39/`.

[2] R. Böttcher, *Geometrical Probabilities of Buffon Type in Bounded Lattices*, Rend. Circ. Mat. Palermo (2) **80**(2008), 31–40.

[3] R. Böttcher, *Geometrical Probabilities with the Principle of Inclusion-Exclusion*, Rend. Circ. Mat. Palermo (2) **81**(2009), 59–68.

[4] A. Duma, M. I. Stoka, *Problems of Buffon Type for the Dirichlet-Voronoi Lattice*, Pub. Inst. Stat. Univ. Paris, 2003, 91–108.

[5] A. Duma, M. I. Stoka, *Problems of Buffon Type with multiple intersections for lattices of parallelograms*, Rend. Circ. Mat. Palermo (2) **78**(2006), 241–248.

[6] L. A. Santaló, *Integral Geometry and Geometric Probability*, Addison-Wesley, London, 1976.

[7] M. I. Stoka, *Problems of Buffon Type for Convex Test Bodies*, Conf. Semin. Mat. Univ. Bari, 1998, 1–17.